small
NANO MICRO
www.small-journal.com

Low-Temperature and Rapid Growth of Large Single-Crystalline Graphene with Ethane

Xiao Sun, Li Lin, Luzhao Sun, Jincan Zhang, Dingran Rui, Jiayu Li, Mingzhan Wang, Congwei Tan, Ning Kang, Di Wei, H. Q. Xu, Hailin Peng and Zhongfan Liu**

Future applications of graphene rely highly on the production of large-area high-quality graphene, especially large single-crystalline graphene, due to the reduction of defects caused by grain boundaries. However, current large single-crystalline graphene growing methodologies are suffering from low growth rate and as a result, industrial graphene production is always confronted by high energy consumption, which is primarily caused by high growth temperature and long growth time. Herein, a new growth condition achieved via ethane being the carbon feedstock to achieve low-temperature yet rapid growth of large single-crystalline graphene is reported. Ethane condition gives a growth rate about four times faster than methane, achieving about 420 μm min^{-1} for the growth of sub-centimeter graphene single crystals at temperature about 1000 °C. In addition, the temperature threshold to obtain graphene using ethane can be reduced to 750 °C, lower than the general growth temperature threshold (about 1000 °C) with methane on copper foil. Meanwhile ethane always keeps higher graphene growth rate than methane under the same growth temperature. This study demonstrates that ethane is indeed a potential carbon source for efficient growth of large single-crystalline graphene, thus paves the way for graphene in high-end electronical and optoelectronical applications.

1. Introduction

In recent years, huge attention has been paid to the industrial-level production of graphene, due to its exceptionally optical, electrical, mechanical, and thermal properties.[1–5] Amongst various synthetic approaches, chemical vapor deposition (CVD) on transition metals, especially on copper, becomes one of the most popular methods, due to its unparalleled advantages in graphene synthesis with high quality and uniformity.[6–8] However, a high density of grain boundaries in polycrystalline graphene film strongly degrades the mechanical and electrical properties of graphene.[9,10] To improve the quality of graphene, great efforts have been made on the growth of large single-crystalline graphene through suppression of graphene nucleation. However, such routes still suffer from the low growth rate of graphene (approximately few micrometers per second), thus the growth of centimeter-sized graphene single crystals requires hours or even several days. CVD growth of graphene on copper foil via methane, which is still one of the most common carbon sources, has a high decomposition energy barrier. After analysis, we found the low growth rate is presumably due to very low production of active carbon species (for instance, methyl radicals, methylene radicals, and methyne radicals) for graphene growth, especially when the catalytic ability of copper is reduced with the increasing coverage of graphene layer. Furthermore, the higher decomposition barrier of methane also requires a higher growth temperature (usually above 1000 °C) for the produce of carbon species. The long-duration of graphene growth and high growth temperature will cause significant energy consumption, resulting in the expensive costs of high quality graphene.

Herein, we present a strategy to reduce energy consumption of growth of large single-crystalline graphene on copper foil by using ethane as carbon source, which has a lower energy barrier to form active carbon species. The key of this route is

X. Sun, Dr. L. Lin, L. Sun, J. Zhang, M. Wang, C. Tan, Prof. H. Peng, Prof. Z. Liu
Center for Nanochemistry
Beijing Science and Engineering Center for Nanocarbons
Beijing National Laboratory for Molecular Sciences
College of Chemistry and Molecular Engineering
Peking University
Beijing 100871, P. R. China
E-mail: hlpeng@pku.edu.cn; zfliu@pku.edu.cn
X. Sun, L. Sun, J. Zhang, J. Li, C. Tan, Prof. H. Peng, Prof. Z. Liu
Academy for Advanced Interdisciplinary Studies
Peking University
Beijing 100871, P. R. China
D. Rui, J. Li, Prof. N. Kang, Prof. H. Q. Xu
Beijing Key Laboratory of Quantum Devices
Key Laboratory for the Physics and Chemistry of Nanodevices
Department of Electronics
Peking University
Beijing 100871, P. R. China
Dr. D. Wei, Prof. H. Peng, Prof. Z. Liu
Beijing Graphene Institute
Beijing 100094, P. R. China

DOI: 10.1002/smll.201702916

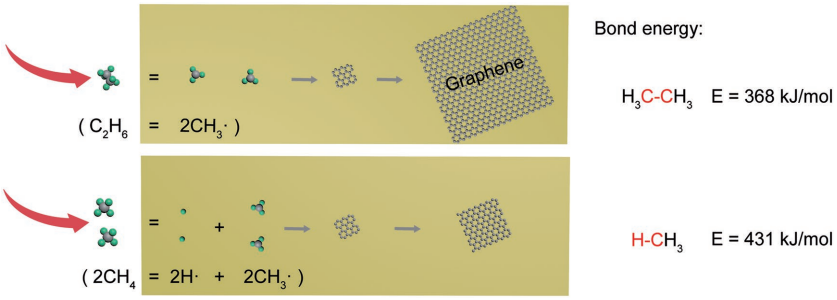

Figure 1. Comparison of ethane and methane source for the rapid growth of large single-crystalline graphene. Schematic illustration of large single-crystalline graphene growth using ethane (up) and methane (bottom) as carbon source, respectively. In detail, the molecular amount of methane introduced is twice of that of ethane. Elementary steps of graphene growth including decomposition of carbon source to form CH_3, nucleation, and domains growth. The bond energies of ethane homolytic reaction and methane dehydrogenation to form CH_3 are as shown above.

that a large amount of methyl radicals could be continuously supplied for graphene growth, when methane was replaced by ethane for the growth of graphene. This allows a significant enhancement in the growth rate of millimeter-size single-crystalline graphene on copper foil with the record high growth rate of 420 μm min^{-1}, much faster than previous reports on pure copper foil.[7,10–19] In addition, the domain of graphene single crystals exceeded 5 mm. We also investigated in the dynamics of graphene growth using ethane with carbon isotope labeling technique, by which indicating that the growth rate of ethane-produced graphene was about four times higher than that of methane-produced graphene. Furthermore, the reduced energy barrier for the decomposition of ethane enabled a lower graphene growth temperature (750 °C) comparing with conventional growth threshold (≈1000 °C) using methane. Moreover, graphene quality as well as growth rate using ethane as feedstock were all higher than that using methane under the same growth temperature.

2. Results and Discussion

The elementary steps of synthesis of graphene on copper foil via CVD method comprise of: (i) the decomposition of carbon source to form active carbon species such as methyl radicals (CH_3), (ii) further on-surface dehydrogenation to form methylene radicals (CH_2) and methyne radicals (CH), (iii) diffusion of such carbon species, (iv) graphene nucleation, and (v) the subsequent growth of graphene.[19–21] The density of nucleation and growth rate of graphene are therefore highly related to the production of carbon species by decomposing carbon source. Clearly, sufficient supply of CH_3 would promise a higher growth rate of graphene. **Figure 1** illustrates the schematic diagram of the comparison in growth process between methane and ethane for the rapid growth of large single-crystalline graphene. When methane is used as carbon precursor, the high-temperature decomposition of methane would result in the formation of CH_3, which would subsequently fuel the nucleation and graphene growth. However, the energy of C—H bond (around 431 kJ mol^{-1}) should be overcome to attain the final formation of CH_3. Such high bond energy would therefore lead to limited carbon precursors for graphene growth, and eventually play a contradictory role on growth rate. By contrast, ethane will promise a highly efficient production of CH_3 due to its lower C—C bond energy (around 368 kJ mol^{-1})[22,23] and enable graphene formation with a higher growth rate (Figure 1). The common growth procedure was presented in Figure S1 (Supporting Information). Ethane and methane with the molecule ratio of 1:2 were used for graphene growth, respectively, which would ensure the same amount of carbon atoms was introduced. Clearly, within the same growth interval, the domain size of graphene grains when ethane is used as carbon source are larger than using methane, by which indicating a faster growth rate (Figure S2, Supporting Information).

Furthermore, during the growth, the amount of active carbon species on copper substrate will determine both nucleation density and growth rate. Larger amount of active carbon species will result in higher nucleation density (more domain boundaries, which will result in lower quality) and faster growth rate, placing a tradeoff between quality and energy consumption. With the same amount of carbon atoms introduced into the system (by control the molecular ratio of ethane to methane is 1:2), the growth of graphene using ethane as carbon source is faster while the nucleation density is slightly higher (Figure S2, Supporting Information). If we change the molecular flow ratio of ethane to methane from 1:2 to 1:3–4, the nucleation density of graphene with ethane or methane will be approximately the same, but ethane-produced graphene single crystals was proved to have a higher growth rate than methane-produced ones (Figure S3, Supporting Information). Consequently, this result clearly displays the superiority of ethane as carbon source in fast growth of large graphene single crystals.

Remarkably, 5 mm graphene single crystals were successfully grown on copper foil using ethane, as shown in **Figure 2**a, which was visualized by heating the copper at 200 °C (see the Supporting Information for growth method). Moreover, large-area continuous graphene film consisted by large single-crystalline graphene domains was successfully synthesized by prolonging the growth time by 40 min and transferred onto a 4 in. Si/SiO_2 wafer (Figure 2b and growth method in the Supporting Information). After the optimization of the pretreatment of copper and the gradually increased feeding of ethane during the growth, a maximum growth rate of 420 μm min^{-1} (Figure 2c) can be attained for growing millimeter-sized graphene single crystals (Figure S4 and growth method in the Supporting Information). This is a significant improvement of growth rate versus previously reported results in terms of growing millimeter-sized graphene domains on copper foil.[10–18]

Transmission electron microscopy (TEM) was conducted to probe the crystallinity of as-grown graphene crystals. One individual square graphene crystal with the domain size of 2 mm was transferred on a TEM grid (Figure 2d). Selected-area electron diffraction (SAED) patterns were collected across the entire domain (inset, Figure 2e; Figure S5, Supporting

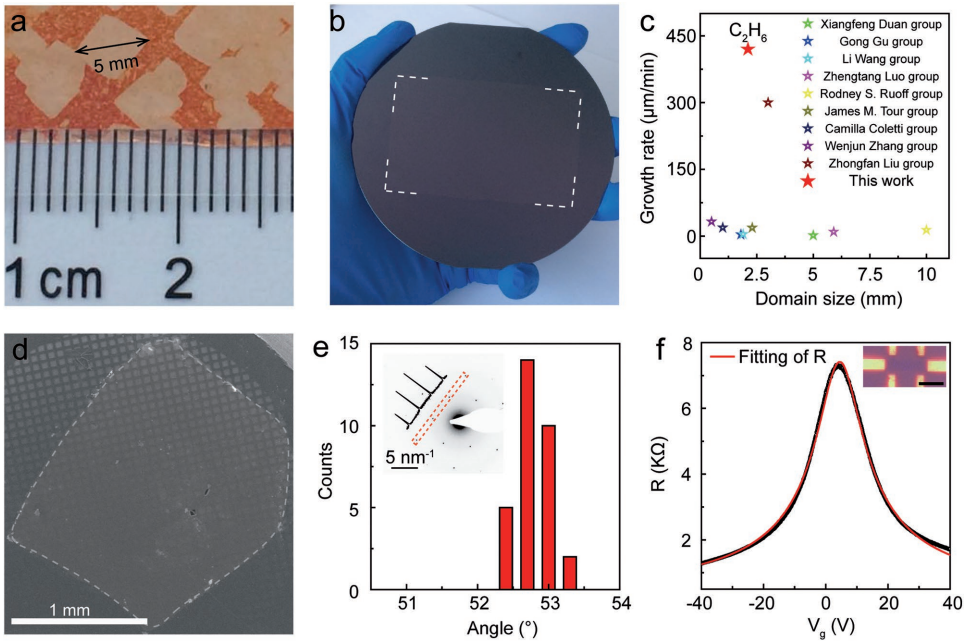

Figure 2. Rapid growth of large single-crystalline graphene using ethane and structural characterizations. a) Photograph of graphene domains grown on copper foil using ethane. The graphene domains became visible after heated the sample in air for 5 min at 200 °C. b) Photograph of the continuous graphene film transferred onto a 4 in. Si/SiO_2 wafer. c) The growth rate of large single-crystalline graphene using ethane comparing with previously reported works. d) SEM image of 2 mm sized single-crystalline graphene transferred onto a TEM grid. e) Histogram of angle distribution from extensive SAED patterns within the graphene domain of (d). Inset: the SAED pattern and the intensity profile of diffraction pattern along the red dashed line. f) Resistance (R) versus back gate voltage (V_g) of the graphene FET device at room temperature. Inset: the OM image of the measured FET device with Hall bar structure. Scale bar: 5 μm.

Information). The distribution of the relative orientations of graphene lattices extracted from extensive SAED patterns was analyzed (Figure 2e; Figure S5, Supporting Information), justifying single-crystalline nature of the graphene domain. Along the dashed line in the SAED pattern, the intensity of inner peaks is stronger than that of outer peaks, indicating the single-layer nature.[24] In addition to TEM, Raman spectroscopy is informative with respect to the identification of graphene layer numbers and evaluation of the quality. Represented Raman spectra of as-grown graphene domains (Figure S6, Supporting Information) display two characteristic G and 2D bands peaks, with a negligible D band intensity, indicating the high-quality and uniformity of monolayer graphene.[25] To evaluate the electrical properties of as-grown graphene, the large graphene film transferred onto a silicon substrate with 300 nm thick silicon oxide, followed by the fabrication into field-effect transistor (FET) devices (inset of Figure 2f). Measurement of these devices at room temperature takes the resistance of the sample as a function of the back gate voltage (V_g) (Figure 2f), which demonstrated a typical ambipolar behavior. The extracted room-temperature carrier mobility from the R (V_g) curve using the nonlinear fitting method[26] is ≈8000 $cm^2\ V^{-1}\ s^{-1}$, which is comparable to previously reported results in single-crystalline graphene on Si/SiO_2,[7,10,11,14,17,18] further justifying the high-quality of as-grown graphene.

To further investigate the growth dynamics and determine the growth rate, ^{12}C-labeled ethane ($^{12}C_2H_6$) and ^{13}C-labeled methane ($^{13}CH_4$) were introduced sequentially and switched every 30 s during the CVD growth process (as decoded in the color bars in **Figure 3**a). To ensure the same number of carbon atoms was introduced for the comparison, $^{12}C_2H_6$ was kept at 2 sccm (standard cubic centimeter per minute) and $^{13}CH_4$ 4 sccm in each growth segment. As-grown graphene domains were transferred onto an Si/SiO_2 substrate for detailed Raman characterization (Figure S7, Supporting Information). Due to the surface-mediated catalytic process of graphene on copper foil, the growth-ring-like pattern distribution of carbon isotope could be used to determine the temporal evolution of ethane- and methane-growth graphene in the same single crystal, which can be visualized by 2D mapping of Raman spectroscopy (Figure 3b) with the different Raman mode frequencies of ^{12}C and ^{13}C.[20,27,28] The line-scan of single-point Raman spectra, which were collected from the center to the edge of the graphene grain, clearly shows the different peak position of isotopic labeling area, corresponding to the pattern distribution of ethane-grown and methane-grown graphene, respectively (Figure 3c). Figure 3d shows that the domain size of graphene as a function of growth time, obtained from the corresponding map. Therefore, the growth rates in different stages were calculated accordingly (Figure 3e). Notably, the growth of ethane-grown graphene is much faster (about four times) than that of methane-produced graphene. Usually, the gradually increased rim length of graphene domains and reduced exposed copper surface will slow down the growth rate, and eventually cease the growth process. In this regard, the temporal evolution of growth rate (Figure 3e) indicates that the decline trend of growth rate of ethane-produced graphene is prominently smaller than that of methane-produced graphene, because the higher decomposition ability of ethane would offset the reduced catalytic ability

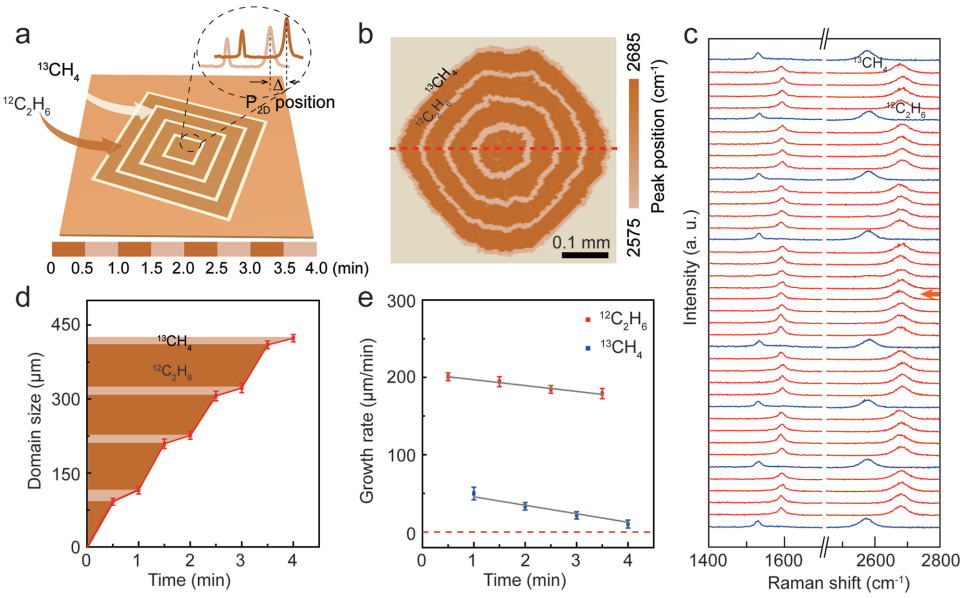

Figure 3. Dynamics of growth of large single-crystalline graphene on copper foils by isotopic-labeling technique in conjunction with micro-Raman spectroscopy. a) Schematic diagram of the carbon isotope labeling process and the separated Raman mode of ^{12}C and ^{13}C in graphene. The dose sequence is decoded in the color bar below, where dark color and the light color represent $^{12}C_2H_6$ and $^{13}CH_4$, respectively. The separated Raman modes of ^{12}C and ^{13}C in graphene basal plane reflected the distribution of $^{12}C_2H_6$ and $^{13}CH_4$. b) Raman 2D-band position map of the as-grown graphene (see Figure S6, Supporting Information). The flux of H_2:$^{12}C_2H_6$:$^{13}CH_4$ is 1000:2:4. c) The single Raman spectra were collected with even space of 15 μm from the center of as-grown graphene, along the red dashed line marked in (b). The red arrow indicates the position of the nucleation center. d) Domain size (diagonal of graphene domains) of as-grown graphene as function of growth time. e) Calculated growth rate of as-grown graphene for every 30 s. The red dashed line indicates zero growth rate. Note that the growth rate of 200 μm min^{-1} was achieved by using C_2H_6, while only 50 μm min^{-1} using CH_4 under this condition.

of copper. Thus, a continuous enhancement of growth would promise an efficient production of high-quality continuous graphene films.

High-temperature is also required during the CVD growth of graphene due to the high bond energies of carbon source and the relatively low catalytic ability of copper, which will lead to the high energy consumption. In comparison with methane, ethane can be dissociated at a relatively lower temperature for the growth of graphene due to lower bond energy of C—C bond. To prove the capability of ethane for growing high-quality graphene at lower temperature, Raman spectroscopy was performed on graphene grown at 950, 900, 850, 800, and 750 °C using ethane and methane, respectively (**Figure 4**a–d; Figures S8 and S9, Supporting Information). Importantly, ethane-produced graphene can still be formed at 750 °C (Figure 4c) with a prominent 2D band in Raman results (Figure 4d). By contrast, when methane is used for graphene growth, no graphene was observed at a growth temperature lower than 900 °C (Figure S9, Supporting Information). In detail, the intensity of D band, stemming from the presence of defects in graphene,[29,30] can be used to reflect the density of defect in graphene lattice. The temperature dependency of intensity ratio of D band to G band (I_D/I_G) of graphene grown using ethane and methane is plotted in Figure 4e, further confirming the better ability of ethane to produce high quality graphene, in comparison with that of methane under same condition. In addition, growth rate of graphene using ethane was still much faster than that using methane as carbon feedstock (Figure 4f). Consequently, a higher growth rate along with a lower threshold of growth temperature can be achieved by using ethane, which is a significant step forward in realizing industrial production of high-quality graphene.

3. Conclusion

In summary, we have successfully developed a strategy to realize the fast growth of sub-centimeter graphene single crystals by using ethane as carbon source. Ethane has been proven to be an efficient carbon feedstock for the rapid growth of high-quality graphene at reduced growth temperature. The growth of sub-centimeter-sized graphene single crystal with a remarkably high growth rate of 420 μm min^{-1} has been achieved, which is much faster than those of previously reported results on copper foil. Besides, in a clear contrast with methane, ethane exhibited relatively weaker reduction in growth rate during the entire growth, which is usually caused by the coverage of graphene. Furthermore, graphene was successfully synthesized at the temperature of 750 °C, which was a much lower working temperature than that of using methane. Meanwhile graphene quality and growth rate using ethane were all superior to that with methane at the same growth temperature. Our work breaks the dilemma of quality versus energy consumption for the growth of graphene, thus paves the way toward the real application of high-quality graphene at an industrial level.

4. Experimental Section

Copper Foil Pretreatment: Commercial available copper foil (98% purity, 25 μm thick, Alfa Aesar #46365) was electrochemically polished

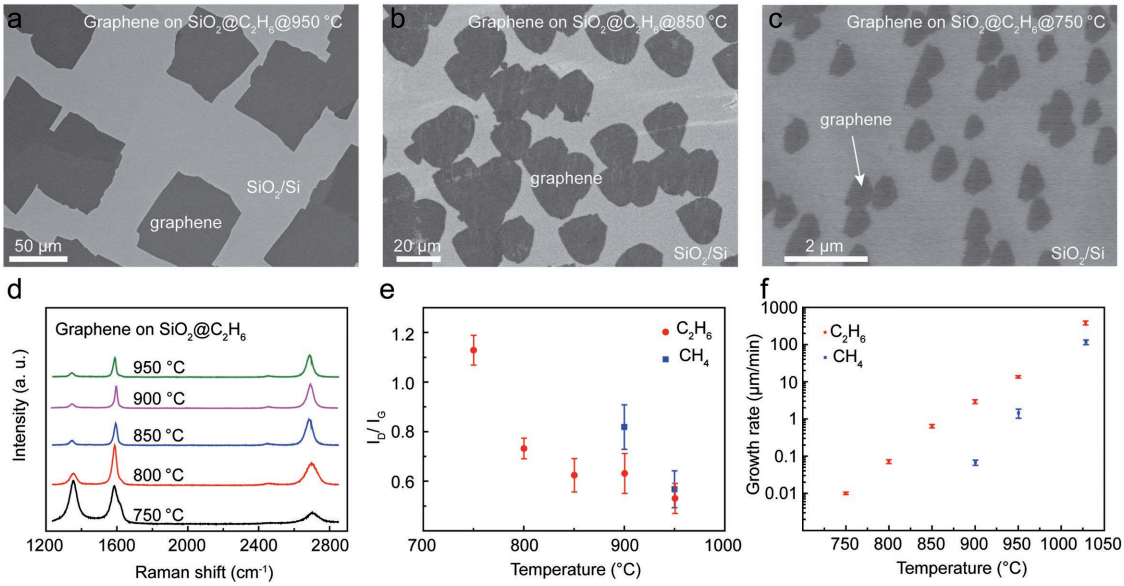

Figure 4. Low temperature growth of graphene using ethane. SEM images of graphene growth with ethane transferred on SiO_2/Si under a) 950 °C, b) 850 °C, and c) 750 °C. d) Raman spectra of as-grown graphene under different temperature. e) The intensity ratio of D peak to G peak of graphene grown with ethane or methane under different growth temperature. f) Graphene growth rate as function of growth temperature. Note that, graphene was successfully synthesized under 750 °C with ethane, while no graphene appeared with methane under temperature lower than 900 °C.

in electrolyte solution composed of phosphoric acid and ethylene glycol (V/V = 3:1) with a bias of 2 V for 30 min to clean the surface. Stacked copper foils[18] were placed in the heating center of the furnace (Lindberg/Blue M), which was equipped with a 1 in. diameter quartz tube and the base pressure of the system was evacuated to about 1 Pa. To promote the monocrystallization of copper foil[18] and to passivate the nucleation sites and reduce the nucleation density,[7] the oxygen assisted annealing process (0.5–1 h) was then conducted, where the stacked copper foils were heated up to 1035 °C with 300–500 sccm Ar/O_2 (V/V = 10000:1) with a pressure of about 200–550 Pa. Then Ar/O_2 was turned off and 100–300 sccm hydrogen (corresponding to a pressure of about 100–500 Pa) was introduced for 5–10 min to remove the adsorbed oxygen of copper foil surface.

Graphene Growth and Isotopic Labeling Process: The graphene growth was initiated by introducing 0.02–2 sccm ethane and maintained for 4–40 min according to the request of samples. Notably, multistage carbon supply was used for the rapid growth of large single-crystalline graphene, where the flux of ethane was stepwise increased with 0.05 sccm every 30 s. In the isotopic labeling process, 4 sccm $^{13}CH_4$ (99% purity, Sigma-Aldrich) and 2 sccm $^{12}C_2H_6$ were sequentially introduced and repeated for four times while the hydrogen was kept with 1000 sccm during the entire process. Finally, the copper foils were rapidly cooled down to room temperature by pulling them out of the high-temperature zone to room temperature without changing the gas flow.

Graphene Transfer: Graphene grown on the inner surfaces of the copper foil stack was transferred onto target substrates with the assistance of polymethyl methacrylate (PMMA) as a transporter. The target graphene grown side of the copper foil after growth was spin-coated with PMMA and then baked in air for 5 min at 200 °C, and then the other side of copper foil was exposed to O_2 plasma for 2 min to remove the graphene on this side. Subsequently, the sample was floated in 1 M $Na_2S_2O_8$ solution to etch the copper foil. Then, the PMMA was dissolved by acetone after graphene/PMMA film was loaded onto SiO_2/Si or TEM grid.

Characterizations: Optical microscopy (OM), scanning electron microscopy (SEM) images, and Raman spectra were obtained on an Olympus BX51 optical microscope, a Hitachi S4800 field-emission scanning electron microscope, and a Horiba HR800 Raman system with 514 nm laser wavelength, respectively. TEM imaging and corresponding SAED were performed with the ultrathin amorphous carbon-covered and lacey carbon film supported copper grids using an FEI Tecnai F30 TEM operated at 300 kV.

Electronic Properties Measurements: After the transfer of the graphene samples onto the SiO_2/Si substrates with predefined markers, atomic force microscopy was employed to ensure the flatness of the samples. Electron beam lithography (EBL) (Raith 150 2nd) and reactive ion etching O_2 etching (Trion technology minilock III) were used to pattern graphene into Hall bar geometry. Titanium/gold (5/90 nm) electrodes were patterned on the graphene samples using standard EBL followed by electron-beam evaporation of the metals (Kurte J. Lesker AXXIS). Electrical transport at room temperature was performed in a vacuum probe station (Lake Shore TTP-4), using Keithley Semiconductor Characterization System (Model 4200-SCS).

Supporting Information

Supporting Information is available from the Wiley Online Library or from the author.

Acknowledgements

X.S. and L.L. contributed equally to this work. This work was financially supported by the National Basic Research Program of China (Nos. 2016YFA0200101, 2013CB932603, and 2014CB932500), the National Natural Science Foundation of China (Nos. 51432002, 51520105003, 21525310, and 51362029), and Beijing Municipal Science & Technology Commission (Nos. Z161100002116002 and Z161100002116021).

Conflict of Interest

The authors declare no conflict of interest.

Keywords

ethane, large single-crystalline graphene, low decomposition energy, low-temperature growth, rapid growth

Received: August 24, 2017
Revised: September 15, 2017
Published online: November 10, 2017

[1] X. Huang, Z. Zeng, Z. Fan, J. Liu, H. Zhang, *Adv. Mater.* **2012**, *24*, 5979.
[2] Y. Zhu, S. Murali, W. Cai, X. Li, J. W. Suk, J. R. Potts, R. S. Ruoff, *Adv. Mater.* **2010**, *22*, 3906.
[3] K. S. Novoselov, V. I. Fal'ko, L. Colombo, P. R. Gellert, M. G. Schwab, K. Kim, *Nature* **2012**, *490*, 192.
[4] G. Eda, G. Fanchini, M. Chhowalla, *Nat. Nanotechnol.* **2008**, *3*, 270.
[5] A. K. Geim, K. S. Novoselov, *Nat. Mater.* **2007**, *6*, 183.
[6] Z. Yan, Z. Peng, J. M. Tour, *Acc. Chem. Res.* **2014**, *47*, 1327.
[7] Y. Hao, M. Bharathi, L. Wang, Y. Liu, H. Chen, S. Nie, X. Wang, H. Chou, C. Tan, B. Fallahazad, *Science* **2013**, *342*, 720.
[8] L. Banszerus, M. Schmitz, S. Engels, J. Dauber, M. Oellers, F. Haupt, K. Watanabe, T. Taniguchi, B. Beschoten, C. Stampfer, *Sci. Adv.* **2015**, *1*, e1500222.
[9] G. H. Han, F. Gunes, J. J. Bae, E. S. Kim, S. J. Chae, H. J. Shin, J. Y. Choi, D. Pribat, Y. H. Lee, *Nano Lett.* **2011**, *11*, 4144.
[10] H. Zhou, W. J. Yu, L. Liu, R. Cheng, Y. Chen, X. Huang, Y. Liu, Y. Wang, Y. Huang, X. Duan, *Nat. Commun.* **2013**, *4*, 2096.
[11] A. Mohsin, L. Liu, P. Liu, W. Deng, I. N. Ivanov, G. Li, O. E. Dyck, G. Duscher, J. R. Dunlap, K. Xiao, *ACS Nano* **2013**, *7*, 8924.
[12] C. Wang, W. Chen, C. Han, G. Wang, B. Tang, C. Tang, Y. Wang, W. Zou, W. Chen, X. A. Zhang, S. Qin, S. Chang, L. Wang, *Sci. Rep.* **2014**, *4*, 4537.
[13] L. Gan, Z. Luo, *ACS Nano* **2013**, *7*, 9480.
[14] S. Chen, H. Ji, H. Chou, Q. Li, H. Li, J. W. Suk, R. Piner, L. Liao, W. Cai, R. S. Ruoff, *Adv. Mater.* **2013**, *25*, 2062.
[15] V. Miseikis, D. Convertino, N. Mishra, M. Gemmi, T. Mashoff, S. Heun, N. Haghighian, F. Bisio, M. Canepa, V. Piazza, *2D Mater.* **2015**, *2*, 014006.
[16] H. Wang, G. Wang, P. Bao, S. Yang, W. Zhu, X. Xie, W. J. Zhang, *J. Am. Chem. Soc.* **2012**, *134*, 3627.
[17] Z. Yan, J. Lin, Z. Peng, Z. Sun, Y. Zhu, L. Li, C. Xiang, E. L. Samuel, C. Kittrell, J. M. Tour, *ACS Nano* **2012**, *6*, 9110.
[18] H. Wang, X. Xu, J. Li, L. Lin, L. Sun, X. Sun, S. Zhao, C. Tan, C. Chen, W. Dang, H. Ren, J. Zhang, B. Deng, A. L. Koh, L. Liao, N. Kang, Y. Chen, H. Xu, F. Ding, K. Liu, H. Peng, Z. Liu, *Adv. Mater.* **2016**, *28*, 8968.
[19] L. Lin, L. Sun, J. Zhang, J. Sun, A. L. Koh, H. Peng, Z. Liu, *Adv. Mater.* **2016**, *28*, 4671.
[20] X. Li, W. Cai, L. Colombo, R. S. Ruoff, *Nano Lett.* **2009**, *9*, 4268.
[21] K. Yan, L. Fu, H. Peng, Z. Liu, *Acc. Chem. Res.* **2013**, *46*, 2263.
[22] Y. R. Luo, *Handbook of Bond Dissociation Energies in Organic Compounds*, CRC Press, Boca Raton, FL, USA **2003**.
[23] J. K. Wassei, M. Mecklenburg, J. A. Torres, J. D. Fowler, B. C. Regan, R. B. Kaner, B. H. Weiller, *Small* **2012**, *8*, 1415.
[24] J. C. Meyer, A. K. Geim, M. I. Katsnelson, K. S. Novoselov, T. J. Booth, S. Roth, *Nature* **2007**, *446*, 60.
[25] A. C. Ferrari, J. C. Meyer, V. Scardaci, C. Casiraghi, M. Lazzeri, F. Mauri, S. Piscanec, D. Jiang, K. S. Novoselov, S. Roth, A. K. Geim, *Phys. Rev. Lett.* **2006**, *97*, 187401.
[26] S. Kim, J. Nah, I. Jo, D. Shahrjerdi, L. Colombo, Z. Yao, E. Tutuc, S. K. Banerjee, *Appl. Phys. Lett.* **2009**, *94*, 062107.
[27] L. Malard, J. Nilsson, D. Elias, J. Brant, F. Plentz, E. Alves, A. C. Neto, M. Pimenta, *Phys. Rev. B* **2007**, *76*, 201401.
[28] L. Sun, L. Lin, J. Zhang, H. Wang, H. Peng, Z. Liu, *Nano Res.* **2017**, *10*, 355.
[29] Z. Ni, Y. Wang, T. Yu, Z. Shen, *Nano Res.* **2010**, *1*, 273.
[30] C. Thomsen, S. Reich, *Phys. Rev. Lett.* **2000**, *85*, 5214.